Heliyon 9 (2023) e21889

Contents lists available at ScienceDirect

Heliyon

journal homepage: www.cell.com/heliyon

Sugarcane leaf polysaccharide exerts a therapeutic effect on cardiovascular diseases through necroptosis

Kaili Sun [a,1], Renyikun Yuan [a,1], Jia He [b], Youqiong Zhuo [a], Ming Yang [b], Erwei Hao [c,d], Xiaotao Hou [c,d], Chun Yao [a,**], Shilin Yang [a], Hongwei Gao [a,*]

[a] College of Pharmacy, Guangxi University of Chinese Medicine, Nanning, 530000, China
[b] State Key Laboratory of Innovative Drug and Efficient Energy-Saving Pharmaceutical Equipment, Jiangxi University of Traditional Chinese Medicine, Nanchang, 330004, China
[c] Guangxi Key Laboratory of Efficacy Study on Chinese Materia Medica/Guangxi University of Chinese Medicine, Nanning, Guangxi, 530001, China
[d] Collaborative Innovation Center for Research on Functional Ingredients of Agricultural Residues/Guangxi University of Chinese Medicine, Nanning, Guangxi, 530200, China

ARTICLE INFO

Keywords:
Sugarcane leaf polysaccharide
Necroptosis
Myocardial ischemia reperfusion
Oxidative stress
RIP1/RIP3/MLKL
Nrf2/HO-1

ABSTRACT

Background: Necroptosis, a novel form of programmed cell death wherein the necrotic morphology is characterized by swelling of the cells, rupture of the plasma membrane, and dysfunction of the organelle, has been always observed in cardiovascular diseases. Sugarcane leaf polysaccharide (SLP) are primary components present in sugarcane leaves that exert cardiovascular protective effects. However, the positive effect of SLP and underlying mechanisms in myocardial ischemia-reperfusion (MI/R) remain unexplored.

Aim: In this study, the protective effects of SLP on MI/R injury were investigated under *in vitro* and *in vivo* conditions.

Methods: The protective effects of SLP on MI/R injury were assessed using tertiary butyl hydrogen peroxide (TBHP)–stimulated-H9c2 cells in the *in vitro* assay and using Sprague Dawley rats in the *in vivo* assay.

Results: In vitro, SLP significantly reversed TBHP-induced H9c2 cell death by inhibiting necroptosis and oxidative stress. SLP exerted antioxidant activity through the Nrf2/HO-1 pathway. SLP suppressed necroptosis by decreasing phosphorylation of RIP1, RIP3, and MLKL in TBHP-stimulated H9c2 cells. *In vivo*, SLP attenuated MI/R injury by decreasing the myocardial infarct area; increasing myeloperoxidase and superoxide dismutase levels; and reducing malondialdehyde, interleukin-6, and tumor necrosis factor-α levels.

1. Introduction

In recent decades, cardiovascular disease has become increasingly prevalent in China and is the leading cause of mortality [1]. Owing to the complexity and multi-mechanisms of cardiovascular disease and its integration with other diseases, the treatment for this disease has become inevitably challenging [2,3]. Myocardial ischemia, a major cause of sudden death, occurs as a result of sharp

* Corresponding author.
** Corresponding author.
E-mail addresses: yaochun111111@163.com (C. Yao), gaohongwei06@126.com (H. Gao).
[1] These authors contributed equally to this work.

https://doi.org/10.1016/j.heliyon.2023.e21889
Received 16 November 2022; Received in revised form 6 October 2023; Accepted 31 October 2023
Available online 4 November 2023

decrease in the coronary artery blood flow to the heart owing to thrombosis or atherosclerosis, leading to cardiovascular disease [4]. Reperfusion, a process by which coronary artery blood flow to the ischemic myocardium is restored, is the most common therapeutic strategy. However, sudden reperfusion to the ischemic myocardium leads to oxidative stress and cell necroptosis, further exacerbating the injury, known as myocardial ischemia reperfusion (MI/R) injury [5–7]. MI/R injury is an intricate pathophysiological process that involves several mechanisms including inflammatory responses, oxidative stress, and cellular apoptosis [8–10]. Myocardial necrosis occurs because of prolonged myocardial ischemia and is therefore an irreversible process. After acute coronary artery occlusion, either partial or complete, the ischemia is restored to normal perfusion for a certain duration, while tissue injury undergoes progressive aggravation. A series of reperfusion-induced traumatic changes in terms of energy metabolism, electrophysiology, myocardial ultrastructure, and cardiac function are more prominent than ischemia-related changes; sometimes, severe cases may result in sudden death. Nevertheless, the mechanisms underlying the pathological development of MI/R injury are currently unclear. Mitochondrial reactive oxygen species (ROS) promote necroptosis and activate various molecular cascades of apoptosis, thereby aggravating MI/R injury [11–13]. Therefore, the management of MI/R injury should involve cessation of the increase in free radical production and necroptosis aggravation.

Necroptosis is a novel form of programmed cell death wherein the necrotic morphology is characterized by swelling of cells, rupture of the plasma membrane, and dysfunction of organelles. This phenomenon involves several biological processes including immune response, inflammation, metabolic abnormalities, and embryonic development [14]. Compared with apoptosis, necroptosis causes fracture of the cytomembrane and the subsequent leakage of cellular contents, thereby triggering inflammation and activating the immune system. Although the mechanisms by which necroptosis occurs remain unclear, several necroptosis-triggered signaling complexes have been unraveled, in which the RIP1/RIP3 necrosome signaling complex is probably the most mature [15]. Necroptosis plays an important role in MI/R injury [16]. Accordingly, inhibition of necroptosis is an alternative potential treatment for MI/R injury. The Nrf2/HO-1 pathway is important for regulating ROS generation, and ROS always result in cellular necroptosis [17,18]. Therefore, effective treatment of MI/R injury involves the reduction of ROS-induced necroptosis and the regulation of the Nrf2/HO-1 signaling pathway [19].

Verapamil (molecular formula: $C_{27}H_{38}N_2O_4$) belongs to class IV antiarrhythmic drugs. It has the potential to reduce the rate of depolarization automaticity in the heart during the diastolic phase by inhibiting calcium ion inflow and to slow down the impulse and electrical conductivity of the sinoatrial node. Moreover, it causes the peripheral blood vessels to dilate, leading to a drop in the blood pressure, thereby controlling the elevated blood pressure. Additionally, this drug can also control the reflex heart rate because of the drop in blood pressure [20]. It has a diastolic effect on the coronary artery by increasing coronary artery blood flow, improving myocardial oxygen supply, and inhibiting platelet aggregation [21]. Therefore, it is often used as a positive control drug in rat myocardial ischemia-reperfusion experiments.

Sugarcane (*Saccharum officinarum* Roxb) is a perennial plant belonging to the family Gramineae; it is mainly cultivated in Guangxi, Guangdong, Fujian, Yunnan, and Taiwan, among which the cultivated amount of sugarcane in Guangxi accounts for more than half of the national quantity [22]. In addition to being an important raw material for sugar production, sugarcane has a high comprehensive utilization value. For example, it can be used as a source for the isolation and production of many metabolites with promising antioxidant potential [23]. Sugarcane leaves contain flavonoids, organic acids, polyphenols, vitamins, polysaccharides, and other chemical components that can be widely used in pharmaceuticals, yeast breeding, and alcohol production [24,25]. Polysaccharides, which exist widely in organisms, constitute the structural components and the energy source for cells; participate in cell recognition and signal transduction; and regulate the metabolism, growth, and development of organisms [26]. Sugarcane leaf polysaccharide (SLP), one of the main components in sugarcane leaves, possesses antioxidant, antitumor, and hypoglycemic effects and exerts therapeutic effects on myocardial infarction in rats [27]. However, thus far, the protective mechanisms of SLP against MI/R injury remain unexplored.

The present study investigated the protective effects of SLP against MI/R injury and the underlying mechanisms *in vitro* and *in vivo*.

2. Materials and methods

2.1. Chemical and reagents

SLP was provided by Hou Xiaotao's research group at the Guangxi University of Chinese Medicine (Nanning, China). (±)-Verapamil hydrochloride was purchased from Shanghai Macklin Biochemical Technology Co., Ltd (Shanghai, China). Tertiary butyl hydrogen peroxide (TBHP), MTT, and 2′,7′-dichlorodihydrofluorescein diacetate ($DCFH_2$-DA) were bought from Sigma-Aldrich (St. Louis, MO, USA). Fetal bovine serum (FBS) and Dulbecco's modified Eagle's medium (DMEM) were obtained from Gibco Laboratories (Grand Island, NY, USA). Interleukin (IL)-6 and tumor necrosis factor (TNF-α) enzyme-linked immunosorbent assay (ELISA) kits were obtained from Neobioscience technology (Shenzhen, China). Superoxide dismutase (SOD), malondialdehyde (MDA), and myeloperoxidase (MPO) detection kits were selected and supplied by Nanjing Jiancheng Bioengineering Institute (Nanjing, China). Bicinchoninic acid protein detection kit was supplied by Thermo Fisher Scientific (Waltham, MA, USA). Furthermore, p-RIP1 (AF7088), RIP1 (AF7877), p-RIP3 (AF7443), RIP3 (AF7942), *p*-MLKL (AF7420), and GAPDH (AF7021) were purchased from Affinity Biosciences (Cincinnati, OH, USA). HO-1 (#70081) and secondary antibody (#7074) were procured from Cell Signaling Technology (Beverly, MA, USA). Nrf2 (ab137550), NQO1 (ab80588), and MLKL (ab196436) were obtained from Abcam (Cambridge, UK).

2.2. Drug preparation

Sugarcane leaf samples (10 g) were ground into 60 mesh coarse powder. For extraction of the powder, 30 times the amount of pure water was used, and the process was repeated thrice at 100 °C for 2 h each time. The total filtrates were concentrated to saturation, after which 80 % ethanol was added to the filtrates. After 12 h, the solution mixture was centrifuged, and the precipitate was collected and then washed several times with ethanol, acetone, and ether. The SLP powder was obtained by vacuum-drying. The SLP concentration was determined as 68 % by phenol-sulfuric acid colorimetry according to a method described previously [28].

2.3. Cell culture

H9c2 cells were obtained from the Cell Bank of the Chinese Academy of Sciences (Shanghai, China) and maintained in an incubator at 37 °C and 5 % CO_2. The cells were cultivated in DMEM supplemented with 10 % FBS and 1 % penicillin/streptomycin. The medium was replenished every 2 days.

2.4. Cell viability assay

Cell viability was detected using the MTT assay. H9c2 cells were seeded in 96-well plates at a density of 3.5×10^3 cells per well overnight. Subsequently, the cells were pretreated with SLP (25, 50, and 100 μg/mL) for up to 3 h before induction with TBHP (50, 100, and 150 μM) for 8 h. Absorbance was then determined at 570 nm using a microplate reader (BioTek, Winkowski, VT, USA).

2.5. LDH release assay

Cell cytotoxicity was detected using a lactate dehydrogenase (LDH) assay kit (Beyotime, Shanghai, China). This test quantifies the LDH released into the culture medium after TBHP-induced cell membrane damage. After treatment, the cell culture medium was analyzed, according to the manufacturer's instructions. Absorbance was determined at 490 nm using a microplate reader (BioTek, Winkowski, VT, USA).

2.6. Detection of ROS level

The ROS level in H9c2 cells was measured by flow cytometry using the FITC channel. Cells were cultured overnight in 12-well plates at a density of 6.0×10^4 cells per well, and subsequently, they were pretreated with SLP (25, 50, and 100 μg/mL) for 3 h and induced with TBHP (100 μM). The ROS-sensitive dye $DCFH_2$-DA (1 μM) was co-incubated with the cells at 37 °C for 30 min. The results were quantified using BD FACS software.

2.7. MMP detection assay

Mitochondrial dysfunction can induce the occurrence of cardiovascular diseases [29]. Mitochondrial membrane potential (MMP) was measured by JC-1 staining. In line with our previous study [30], H9c2 cells were cultured overnight in 96-well plates at a density of 4×10^3 cells per well. After treatment, JC-1 (5 μg/mL) was co-incubated with the cells at 37 °C for 1 h. After staining, a fluorescence microscope was used to capture images.

2.8. Immunofluorescence assay

H9c2 cells were cultured overnight in confocal dishes at a density of 6.0×10^4 cells in each well and then pretreated with 100 μg/mL SLP for 3 h and stimulated with 100 μM TBHP for 8 h. After fixation, punching, and blocking, cells in the dishes were incubated overnight with Nrf2 antibody (1:500 dilution) at 4 °C. Finally, the cells were co-incubated with a secondary antibody (AlexaFluor 488). Hoechst 33342 staining was performed to detect the nuclei. Fluorescence images were captured under a confocal microscope.

2.9. Animal experiments

The Laboratory Animal Management Ethics Committee of Guangxi University of Traditional Chinese Medicine has approved license to this study (approval number: DW20220526-115). According to the Guidelines for the Care and Use of Laboratory Animals of the Guangxi University of Traditional Chinese Medicine, all animals were taken care of humanely. Hunan Saike Jingda Experimental Animal Co., Ltd (Changsha, China), supplied healthy male Sprague Dawley (SD) rats (180–200 g), which were acclimated for 1 week. Under controlled conditions of suitable temperature (25 °C) and humidity (50 %), the rats were reared under standard specific-pathogen-free environmental conditions with a 12:12 h light-dark cycle, wherein they had free access to water and diet.

2.10. Establishment of the MI/R SD rat model

Chloral hydrate (10 %; 4 mL/kg) was intraperitoneally injected to rats for anesthesia induction. After successful induction of anesthesia, all rats were subjected to immobilization of the limbs and underwent endotracheal intubation with a needle. The needle

was connected to a ventilator specific for small animals. The third and fourth ribs were cut open to leave the heart almost completely exposed. The left anterior descending (LAD) coronary artery was ligatured at the distal one-third with 6-0 silk suture, which resulted in the paleness of the apex of the heart promptly. After occlusion for 30 min, the ligation was disengaged, and reperfusion was performed for 2 h [31]. BL-420 N biological signal acquisition and analytical system (Chengdu, China) was used to monitor and record electrocardiogram (ECG) changes throughout the experiment.

2.11. Treatments

Conventionally, the SD rats were randomly and uniformly distributed into five groups: (1) sham-operated group: the rats were pretreated with an equal amount of 0.9 % normal saline (NS) at the corresponding time, and after being anesthetized, they were sutured under the LAD coronary artery without blocking. (2) MI/R group: the rats received 0.9 % NS at the corresponding time and the LAD coronary artery was sutured and occlusion was restored. (3) SLP-L group: the rats received SLP (10 mg/kg) by gavage intraperitoneally once daily and the LAD coronary artery was sutured and occlusion was restored; (4) SLP-H group: the rats received SLP (20 mg/kg) by gavage intraperitoneally once daily and the LAD coronary artery was sutured and occlusion was restored; and (5) the positive control medicine verapamil hydrochloride (Ver) group: the rats received Ver (20 mg/kg) by gavage intraperitoneally once daily and the LAD coronary artery was sutured and occlusion was restored. The drugs were pre-administered for 1 week ahead of modeling. The coronary artery was occluded for up to 30 min, followed by reperfusion for 2 h. After reperfusion, blood samples were collected from the abdominal aorta.

2.12. Hematoxylin & eosin (H&E) staining

The heart tissue was harvested and sequentially fixed with 4 % paraformaldehyde and embedded in paraffin. The embedded tissue was sliced into 4-mm-thick sections, after which they were dewaxed and hyalinized with alcohol and xylene at a gradient of concentration. Hematoxylin solution was then used to stain the nucleus, and the eosin solution was used to stain the cytoplasm. Histopathological examination was performed using an optical microscope (DSZ5000X; UOP, China) to observe the pathological changes in the heart tissue slices.

2.13. Determination of myocardial infarct size

Both Evans blue and TTC (2,3,5-triphenyltetrazolium chloride) were used to stain and measure the myocardial infarct area (INF). After reperfusion, 1.5 mL of 1 % Evans blue staining was injected into the femoral vein. As an iconic manifestation, the right side of the heart tissue appeared blue, after which it was immediately removed and washed with NS. After processing, the sample was stored at a low temperature. The heart was sectioned (2 mm) and then incubated with 2 % TTC at 37 °C for 20 min. Biopsies that stained red with TTC indicated areas at risk (AARs). The nonischemic myocardium appeared dark blue when stained with Evans blue. The INF appeared pale after staining. The infarct size was evaluated as a percentage of INF over AAR (INF/AAR%).

2.14. Determination of SOD, MDA, MPO, IL-6, and TNF-α

Immediately after harvesting, the heart tissue was stored at −80 °C and was homogenized using a tissue grinder. According to the manufacturer's instructions, the levels of SOD, MDA, and MPO were measured using the corresponding kits [32,33]. IL-6 and TNF-α levels were determined using the corresponding ELISA kits.

2.15. Western blotting analysis

In vitro, H9c2 cells were cultured overnight in a dish and pretreated with SLP (25, 50, and 100 μg/mL) for 3 h and subsequently with TBHP for 8 h. *In vivo*, the heart tissue was harvested to detect relevant protein expression. Total protein was extracted from the cells and heart tissues using radioimmunoprecipitation assay buffer with 1 % phenylmethylsulfonyl fluoride and 1 % cocktail. Total protein concentration was determined using the bicinchoninic acid kit, according to the manufacturer's instructions. After denaturing, the proteins were separated using 10 % sodium dodecyl sulfate–polyacrylamide gel electrophoresis and subsequently transferred from the gel onto a polyvinylidene difluoride (PVDF) membrane (Millipore, Billerica, MA, USA). Then, 5 % skim milk was used to block the PVDF membrane for 2 h to prevent nonspecific antigen–antibody binding. The membrane was incubated with primary antibodies (1:1000 dilution) at 4 °C for 12 h. The membranes were washed with Tris-buffered saline containing Tween 20 three times and then incubated with secondary antibodies (1:5000 dilution) for 2 h at room temperature, after which ChemiDoc™ MP Imaging System (Bio-Rad, Hercules, CA, USA) was used to detect antibodies in the membrane. GAPDH was used as the housekeeping protein and Lamin B1 was used as a housekeeping protein in the nucleus.

2.16. Statistical analysis

Every experiment was repeated at least three times. All data were normally distributed and expressed as mean ± standard deviation. One-way analysis of variance or Student's *t*-test was performed using GraphPad Prism 6.0 software. When $p < 0.05$, the results were considered to be statistically significant.

3. Results

3.1. SLP attenuated TBHP-stimulated cell death in H9c2 cells

MTT was used to detect the toxicity of SLP. Cell viability showed no significant difference between the SLP group (25, 50, and 100 μg/mL) and the control group (Fig. 1A). Cells were induced with different concentrations of TBHP (50, 100, and 150 μM) to mimic MI/R injury. Compared with the control group, cell viability in the 100 μM and 150 μM TBHP groups was significantly decreased (Fig. 1B), wherein 100 μM TBHP was used to stimulate cells. To detect the effect of SLP, H9c2 cells were pretreated with different concentrations of SLP and then exposed to 100 μM TBHP. SLP attenuated TBHP-stimulated cell death in a dose-dependent manner (Fig. 1C). SLP reversed TBHP-stimulated LDH release in H9c2 cells (Fig. 1D).

3.2. SLP mitigated TBHP-induced ROS generation and MMP loss in H9c2 cells

Under diversified pathological circumstances, ROS can cause cardiac dysfunction, which is suggestive of mitochondrial oxidative stress. For this reason, the $DCFH_2$-DA probe was used to monitor ROS levels. TBHP can induce a sharp augment of ROS levels and promote oxidative stress [34]. ROS generation was determined using the flow cytometry assay. TBHP caused a surge of the ROS level when H9c2 cells were stimulated for 1 h, and SLP evidently suppressed TBHP-stimulated ROS generation (Fig. 2A and B). To conclude, SLP reversed TBHP-induced oxidative stress.

MMP plays a critical physiological role in the energy storage process by oxidative phosphorylation, and its decrease suggests mitochondrial dysfunction [35]. TBHP led to MMP destabilization and was not conducive to the maintenance of regular physiological activities of cells [36]. After MMP detection through JC-1 staining, the image of $H9c_2$ cells was viewed using a fluorescence microscope. The results clearly indicated that, under physiological conditions, JC-1 existed in the mitochondria of cells in the form of polymer and appeared with a bright red fluorescence; however, after TBHP exposure, the JC-1 did not appear as a polymer in the mitochondrial matrix [37]. Therefore, the intensity of the red fluorescence had significantly reduced, whereas the intensity of the green fluorescence had enhanced significantly in the cytoplasm. In cells pretreated with SLP (100 μg/mL), the fluorescence intensity

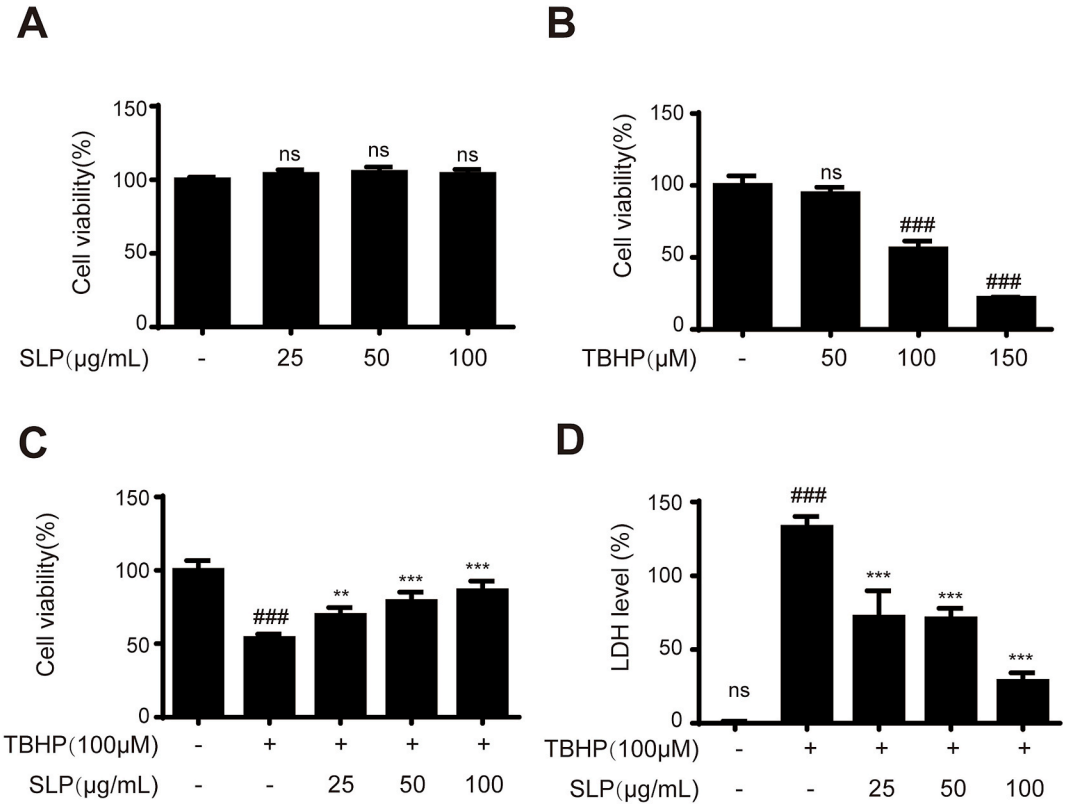

Fig. 1. SLP attenuated TBHP-stimulated cell death and LDH release in H9c2 cells. (A) Cell viability of H9c2 cells was determined by MTT after cells were treated with SLP at a series of concentrations up to 24 h. (B) Cell viability of H9c2 cells was measured by MTT after cells were treated with TBHP for a series of concentrations up to 8 h. (C) Cell viability of H9c2 cells was detected by MTT after cells were pretreated with SLP for 3 h and then exposed to TBHP for 8 h. (D) The LDH release level was detected by LDH kit after treatment. n = 3. $^{ns}p > 0.05$, $^{###}p < 0.001$, vs. the control group. $^{**}p < 0.01$, $^{***}p < 0.001$, vs. TBHP group.

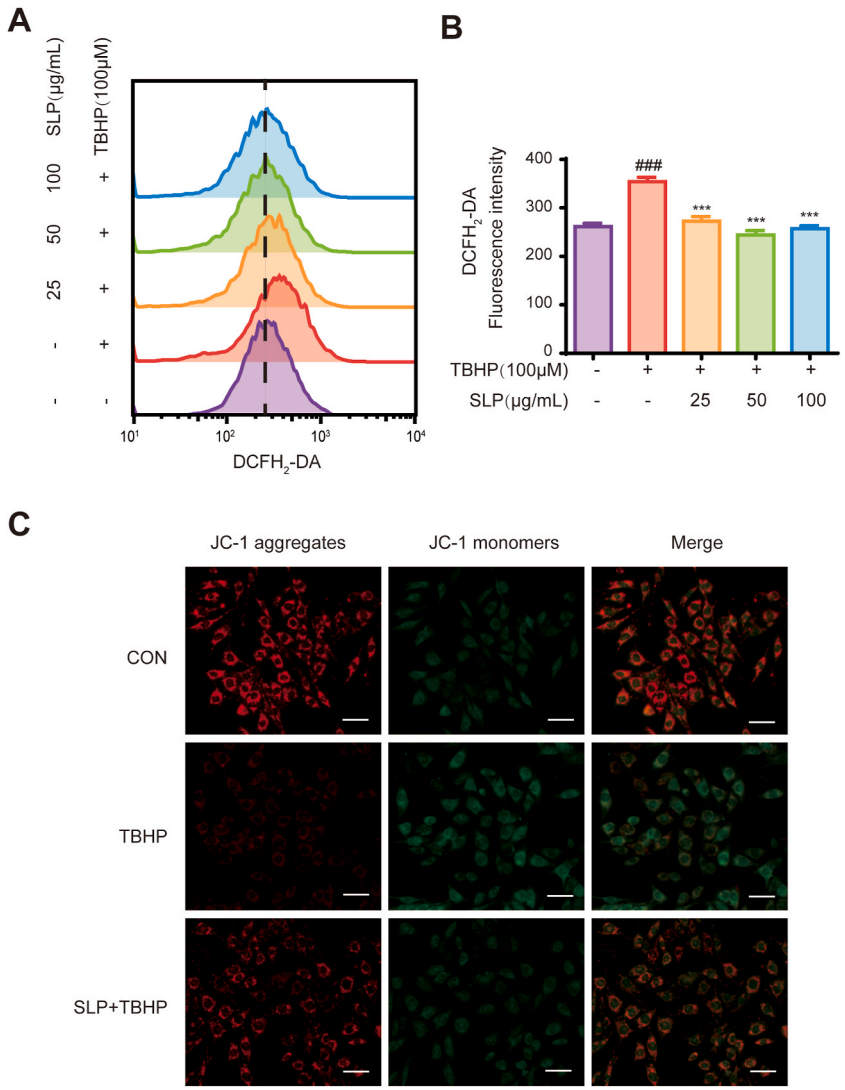

Fig. 2. SLP mitigated TBHP-induced ROS generation and MMP loss detected by flow cytometry and fluorescence microscopy images. (A) Cells were pretreated with SLP (25, 50, and 100 μg/mL) for 3 h and stimulated with TBHP (100 μM) for 1 h. Afterward, H9c2 cells were stained with $DCFH_2$-DA (1 μM) for 30 min to monitor ROS level. (B) Statistical analysis of the ROS level in each group. (C) Pretreated with SLP (100 μg/mL) for 3 h and stimulated by TBHP (100 μM) for 2 h, H9c2 cells were stained with JC-1 (5 μg/mL) for 1 h and relevant photographs were captured under a fluorescence microscope. Scale bar: 5 μm, n = 3. $^{###}p < 0.001$, vs. the control group. $^{***}p < 0.001$, vs. TBHP group.

was markedly reversed (Fig. 2C). Collectively, SLP (100 μg/mL) could rescue TBHP-stimulated elevated ROS levels and MMP loss.

3.3. SLP activated the Nrf2/HO-1 signaling pathway to mitigate oxidative stress injury

The Nrf2/HO-1 signaling pathway plays a vital role in mitigating oxidative stress. Nrf2, a nuclear transcription factor, cooperatively modulates the elementary and derivable expression of antioxidant enzymes and phase 2 detoxification enzymes including HO-1 and NQO-1 [17,38,39]. The results indicated that SLP remarkably promoted the protein expression of Nrf2, HO-1, and NQO-1 (Fig. 3A–D). SLP mitigates oxidative stress injury by increasing the expression of antioxidant proteins.

MDA is a product of lipid peroxidation with cytotoxicity and reflects the potential antioxidant ability of the body. It is not only directly related to the intensity and rate of lipid peroxidation but also indirectly related to the degree of damage due to tissue peroxidation. Compared with the control group, MDA levels in the TBHP group evidently increased and SLP reversed these effects (Fig. 3E).

SLP upregulated nuclear translocation of Nrf2. The transcription factor Nrf2 regulates the expression of antioxidant genes including HO-1 [40]. To investigate the particular mechanism by which SLP exerts protective effects to mitigate oxidative stress through the Nrf2/HO-1 signaling pathway, western blotting and immunofluorescence analyses were performed to monitor the nuclear

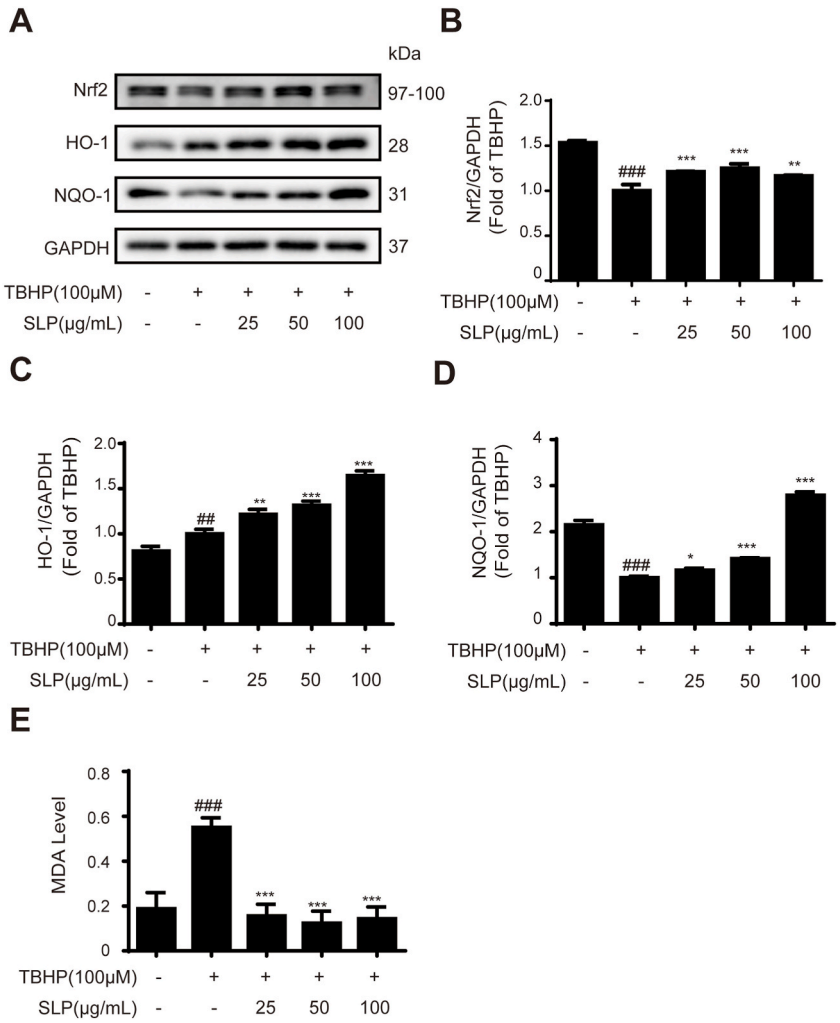

Fig. 3. SLP mitigated oxidative stress through the Nrf2/HO-1 signaling pathway in H9c2 cells. (A) H9c2 cells were pretreated with SLP (25, 50, and 100 μg/mL) for 3 h, respectively, and then exposed to TBHP (100 μM) for 8 h. The expression of Nrf2, HO-1, and NQO-1 proteins was detected by using western blotting. (B–D) Statistical analysis of protein expressions of Nrf2, HO-1, and NQO-1. (E) MDA level in each group was determined using MDA kits. n = 3. $^{\#\#}p < 0.01$, $^{\#\#\#}p < 0.001$, vs. the control group. ***$p < 0.001$, vs. TBHP group.

translocation of Nrf2. SLP promoted the translocation of Nrf2 from the cytoplasm into the nucleus, which suggested that SLP activated Nrf2 and occupied an important position against oxidative stress (Fig. 4A and B). Compared with the TBHP stimulation group, the SLP group showed increased expression of the Nrf2 protein in the nucleus but reduced expression in the cytoplasm, consistent with the results of immunofluorescence analysis (Fig. 4C).

3.4. SLP alleviated TBHP-stimulated cell necroptosis through the RIP1/RIP3/MLKL signaling pathway

The RIP1/RIP3/MLKL signaling pathway is involved in the regulation of necroptosis [41]. Compared with the control group, TBHP promoted phosphorylation of RIP1, RIP3, and MLKL, while SLP reversed this effect (Fig. 5A–D). In conclusion, SLP ameliorated TBHP-stimulated necroptosis.

3.5. SLP attenuated MI/R injury and ameliorated cardiac function in SD rats

ECG was used to monitor the cardiac function of rats in each stage of MI/R injury. Ischemia resulted in the apparent elevation of ST segment in all rats, but reperfusion gradually reduced it (Fig. 6A). Compared with the MI/R group, ECG of the SLP-treatment group and Ver-treatment group taken after 2 h showed that reperfusion ameliorated the condition. The degree of damage due to myocardial tissue peroxidation was assessed using H&E staining. The results indicated that the sham-operated group showed normal observations, indicated by the absence of bleeding or neutrophil infiltration. However, the myocardium was severely damaged after MI/R injury at

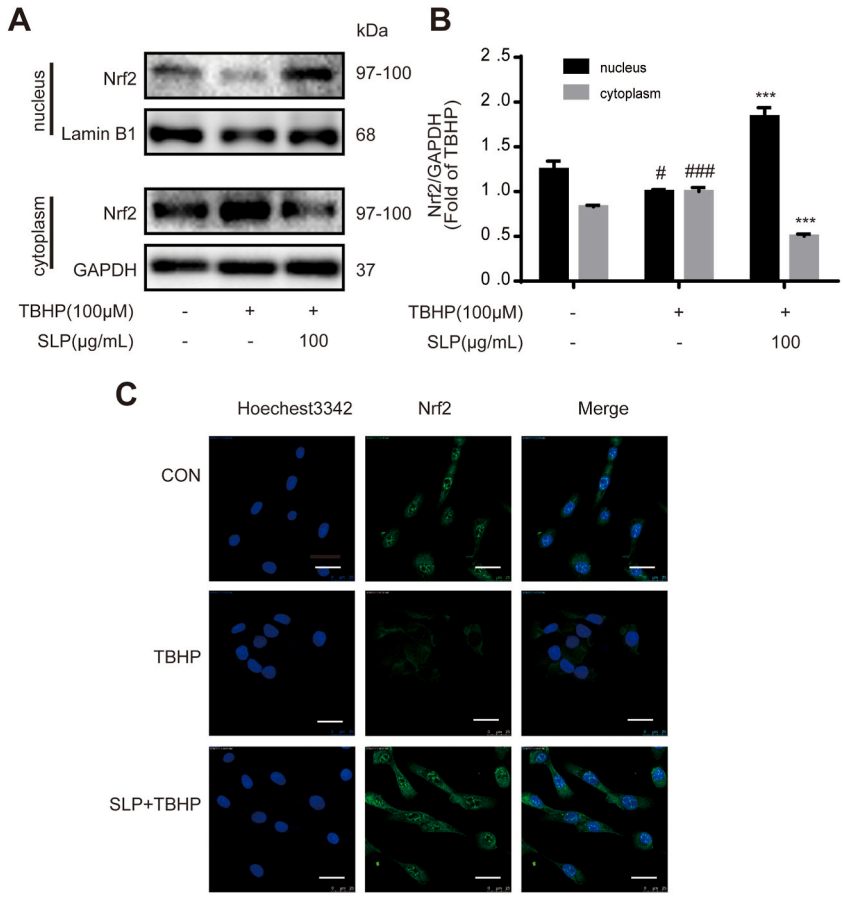

Fig. 4. SLP upregulated the nuclear translocation of Nrf2 in H9c2 cells. (A) H9c2 cells were incubated with SLP (100 μg/mL) and treated with TBHP (100 μM), and the nucleus and cytoplasmic protein expression of Nrf2 was determined using western blotting. (B) Statistical analysis was performed with the data of protein expression in the nucleus and cytoplasm. (C) Nuclear translocation of Nrf2 was detected, and photographs of immunofluorescence analysis results were captured. n = 3. $^{\#}p < 0.05$, $^{\#\#\#}p < 0.001$, vs. the control group. *p < 0.05, **p < 0.01, ***p < 0.001, vs. TBHP group.

the ischemic area, where myocardial fibers dissolved and congregated with inflammatory cells such as neutrophils. SLP and Ver recovered myocardial injury resulting from MI/R (Fig. 6B). To evaluate the protective effect of SLP on MI/R injury, we performed Evans blue and TTC double staining to measure the myocardial infarct size. Compared with the MI/R group, the SLP-L and SLP-H groups showed a significant decrease in the INF/AAR ratio, which suggested that SLP could diminish the myocardial infarct area (Fig. 6C and D).

3.6. SLP inhibited oxidative stress and inflammatory cytokine release in SD rats

The mechanism of MI/R injury involves neutrophil infiltration, calcium overload, energy metabolism disorder, and other theories, among which the oxidative stress theory is the current hotspot topic of research [42,43]. In this study, MI/R decreased SOD activity and improved MDA and MPO activity, but SLP pretreatment reversed these effects (Fig. 7A–C). Additionally, TNF-α and IL-6, which are inflammatory cytokines in the heart tissue that are detected using ELISA kits, showed elevated levels after MI/R injury, while SLP (10 and 20 mg/kg) could reduce the levels of these cytokines (Fig. 7D and E).

3.7. SLP alleviated MI/R injury by diminishing oxidative stress

The Nrf2/HO-1 signaling pathway was found to play a crucial role in the treatment of MI/R injury by diminishing oxidative stress [44,45]. SLP activated the Nrf2/HO-1 signaling pathway to reduce oxidative stress–induced MI/R injury. SLP increased MI/R injury–induced protein expression of Nrf2, HO-1, and NQO-1 (Fig. 8).

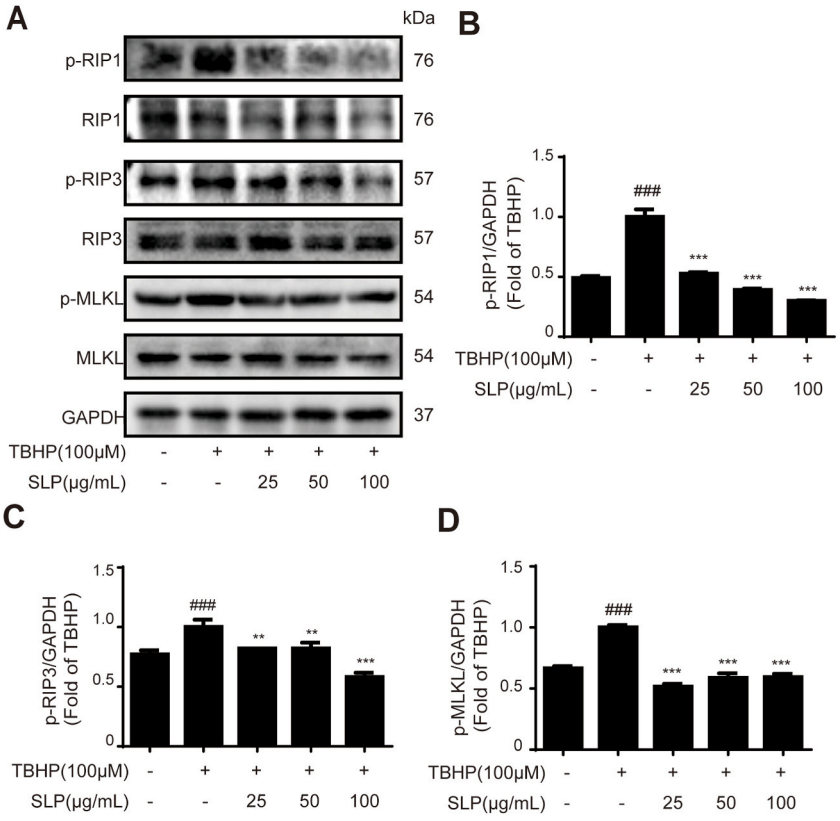

Fig. 5. SLP alleviated TBHP-stimulated cell necroptosis through the RIP1/RIP3/MLKL signaling pathway in H9c2 cells. (A) H9c2 cells were incubated with SLP (25, 50, and 100 μg/mL) and then treated with TBHP (100 μM). The protein expression of p-RIP1, RIP1, p-RIP3, RIP3, *p*-MLKL, and MLKL was determined using western blotting. (B–D) Statistical analysis of the above protein expressions. n = 3. $^{\#\#}p < 0.01$, $^{\#\#\#}p < 0.001$, vs. the control group. $^{*}p < 0.05$, $^{**}p < 0.01$, $^{***}p < 0.001$, vs. TBHP group.

3.8. SLP ameliorated MI/R injury by diminishing myocardial necroptosis

The *in vitro* study indicated that SLP reversed cell necroptosis through the RIP1/RIP3/MLKL signaling pathway. *In vivo*, SLP recovered MI/R-induced necroptosis by reducing phosphorylation of RIP1, RIP3, and MLKL proteins (Fig. 9).

4. Discussion

MI/R injury, an immanent response to reperfusion after ischemia, is an intricate pathological process involving multiple mechanisms within and outside the cellular environment, some of which are modulated by ROS [46]. The main sources of ROS are mitochondrial oxidation, unsaturated fatty acid oxidation, and cytochrome oxidase. When the balance between ROS production and clearance is disturbed, cells undergo irreversible damage, eventually undergoing apoptosis and necroptosis [47]. TBHP is a good alternative to unstable H_2O_2 and is an organic peroxide that is widely used in various studies on oxidative stress to determine ROS release, and it causes damage due to oxidative stress [48]. The significant increase in intracellular ROS leads to cellular necrosis [49,50]. Thus far, the role of TBHP stimulation in oxidative stress and cell necroptosis has rarely been explored.

In fact, the Nrf2/HO-1 signaling pathway plays a crucial role in the treatment of oxidative stress [51]. Nrf2 cooperatively regulates the elementary and derivable expression of antioxidant and phase 2 detoxification enzymes including HO-1 and NQO-1. HO-1, a target gene of Nrf2, regulates the production and elimination of cellular ROS [52,53]. NQO-1 has a potent antioxidant effect and exerts a cytoprotective function [54]. During oxidative stress, Nrf2 is dissociated from Keap-1 and transported to the nucleus, where it combines with antioxidant response element (ARE) and regulates the transcription of ARE-dependent phase II and antioxidant defense enzymes, which include NAD(P)H: quinone acceptor oxidoreductase 1 (NQO-1) as well as heme oxygenase 1 (HO-1). In this way, the Nrf2/HO-1 signaling pathway reduces cellular oxidative stress [55]. In TBHP-induced H9c2 cell death and in the MI/R injury rat model, the expression levels of the Nrf2, HO-1, and NQO-1 proteins reduced evidently, consistent with the results of a previous study [44]. Yet, both *in vitro* and *in vivo* results showed increased expression levels of Nrf2, HO-1, and NQO-1 proteins with SLP pretreatment.

Necroptosis, a novel form of programmed cell death, is mainly regulated by the receptor-interacting protein kinases RIP1 and RIP3 and the mixed lineage kinase domain–like protein MLKL. The RIP1/RIP3/MLKL signaling pathway plays a vital role in regulating various physiological processes and is related to myocardial damage [36,37]. When necroptosis is induced and activated, the complex

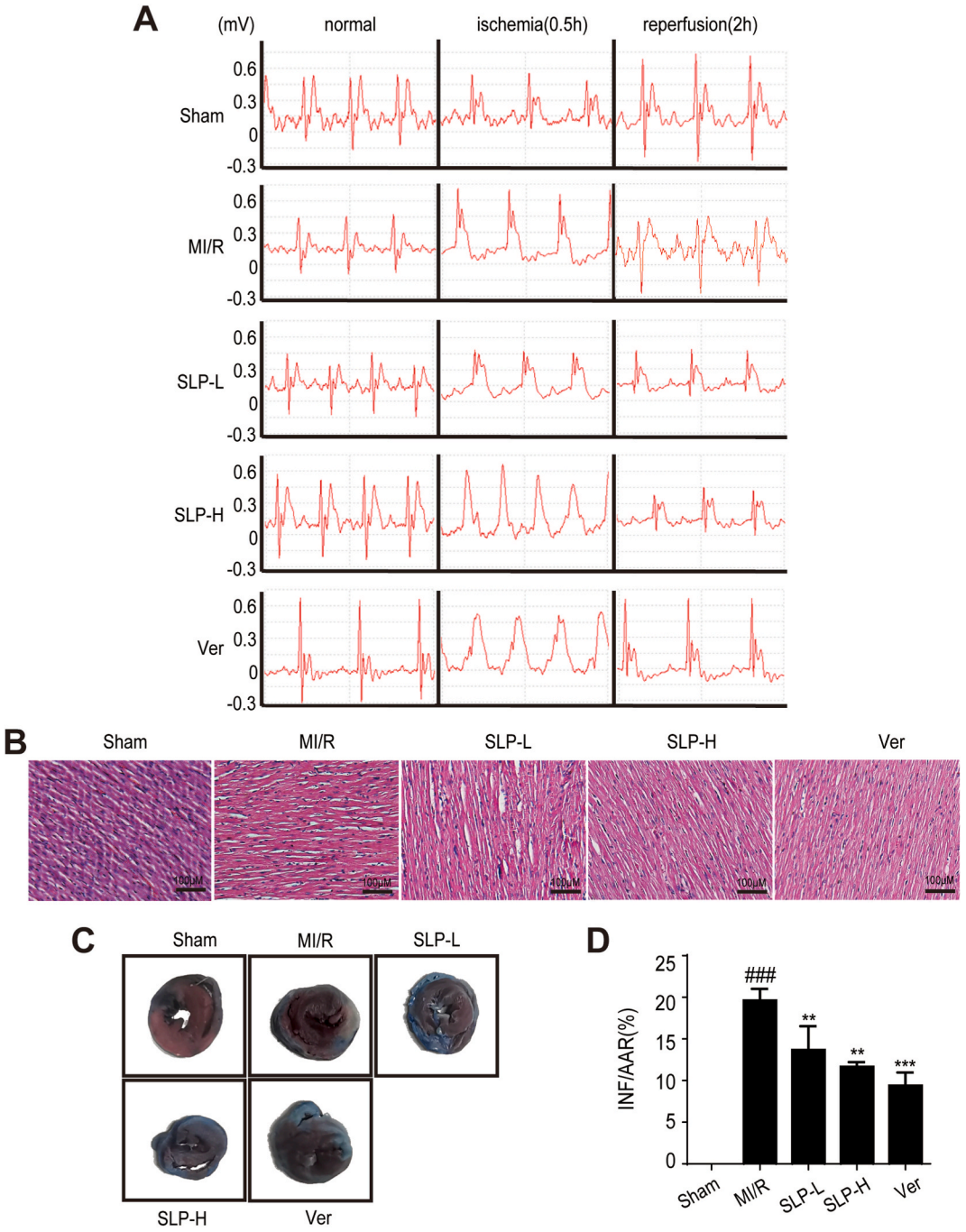

Fig. 6. SLP attenuated MI/R injury and ameliorated cardiac function in SD rats. (A) Representative ECG records in each group. (B) H&E staining for the determination of the injury degree of the rat myocardial tissue. (C) Iconic images were presented: normal area (blue), area at risk (AAR: red and white), and the infract area (INF: white). (D) The infarct area and INF/AAR ratio were quantitatively analyzed. Scale bar: 100 μm n = 3, $^{###}p < 0.001$, vs. sham group. $^{*}p < 0.05$, $^{**}p < 0.01$, $^{***}p < 0.001$, vs. MI/R group. (For interpretation of the references to color in this figure legend, the reader is referred to the Web version of this article.)

formed by RIP1/RIP3 initiates the downstream signal transduction involving MLKL, and then the MLKL signaling factor is phosphorylated and oligomerized by RIP3 and then translocated to the plasma membrane to stimulate necroptosis [52]. Therefore, this study explored the expression of this signaling pathway in MI/R injury. RIP1, RIP3, and MLKL proteins were significantly phosphorylated in both TBHP-stimulated H9c2 cell death and the MI/R injury SD rat model. However, SLP treatment significantly reversed this effect *in vitro* and *in vivo*.

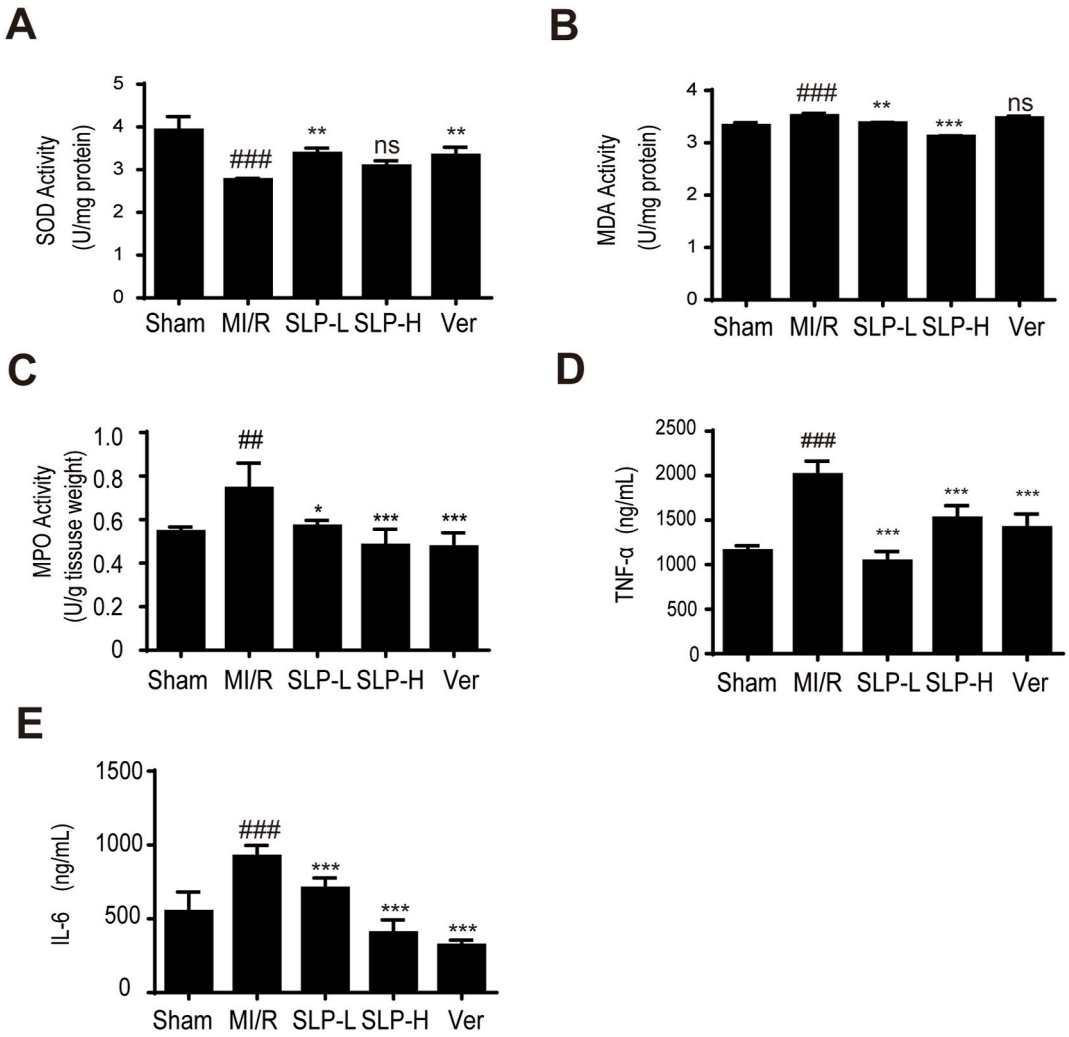

Fig. 7. SLP inhibited oxidative stress and inflammatory cytokine release in SD rats. (A–C) SOD activity, MDA level, and MPO activity were determined using SOD, MDA and MPO kits. (D, E) TNF-α and IL-6 levels in the heart issue were determined by corresponding ELISA kits. n = 5, $^{ns}p > 0.05$, $^{*}p < 0.05$, $^{**}p < 0.01$, $^{***}p < 0.001$, vs. MI/R group. $^{\#\#}p < 0.01$, $^{\#\#\#}p < 0.001$, vs. the sham group.

SLP is a polysaccharide component present in sugarcane leaves. Accumulating evidence suggests that SLP possesses antioxidant activity and can prevent cardiovascular diseases including myocardial infarction and diabetic cardiomyopathy. In our study, SLP could promote the transfer of Nrf2 from the cytoplasm to the nucleus by activating the Nrf2/HO-1 signaling pathway. The antioxidant and detoxification enzymes (Nrf2, HO-1, and NQO-1 proteins) showed upregulated expression and could reduce ROS production and diminish oxidative stress injury. Excess ROS levels affected mitochondrial performance by reducing MMP, which could be mitigated by SLP treatment (100 μg/mL). *In vivo*, SLP effectively reversed MI/R injury in rats, prevented myocardial fibrinolysis and neutrophil infiltration, improved SOD activity in the myocardial tissue, decreased the activity of MDA and MPO induced by MI/R injury, and significantly inhibited TNF-α and IL-6 levels. To prevent the myocardium from undergoing injury due to operated treatment, SLP treatment can be used to obtain a preventive effect. In this study, SLP exerted an evident protective function in alleviating MI/R injury.

This study has some limitations, which should be considered. The H9C2 cells in the *in vitro* experiments did not fully reflect the H9C2 cells in the *in vivo* experiments, and pretreatment with SLP to the MI/R rat model also had some limitations. However, the findings of the present study suggest that oxidative stress and necroptosis could be potential targets in clinical therapy in patients with myocardial infarction refusion or used in early diagnosis by detecting the related gene and protein expression of molecules involved in oxidative stress and necroptosis in the serum of patients with myocardial infarction.

5. Conclusions

This study demonstrated that SLP alleviated oxidative stress and necroptosis by modulating the Nrf2/HO-1 and RIP1/RIP3/MLKL signaling pathways (Fig. 10). In the *in vitro* experiment, SLP alleviated TBHP-stimulated cell necroptosis, MMP loss, ROS generation,

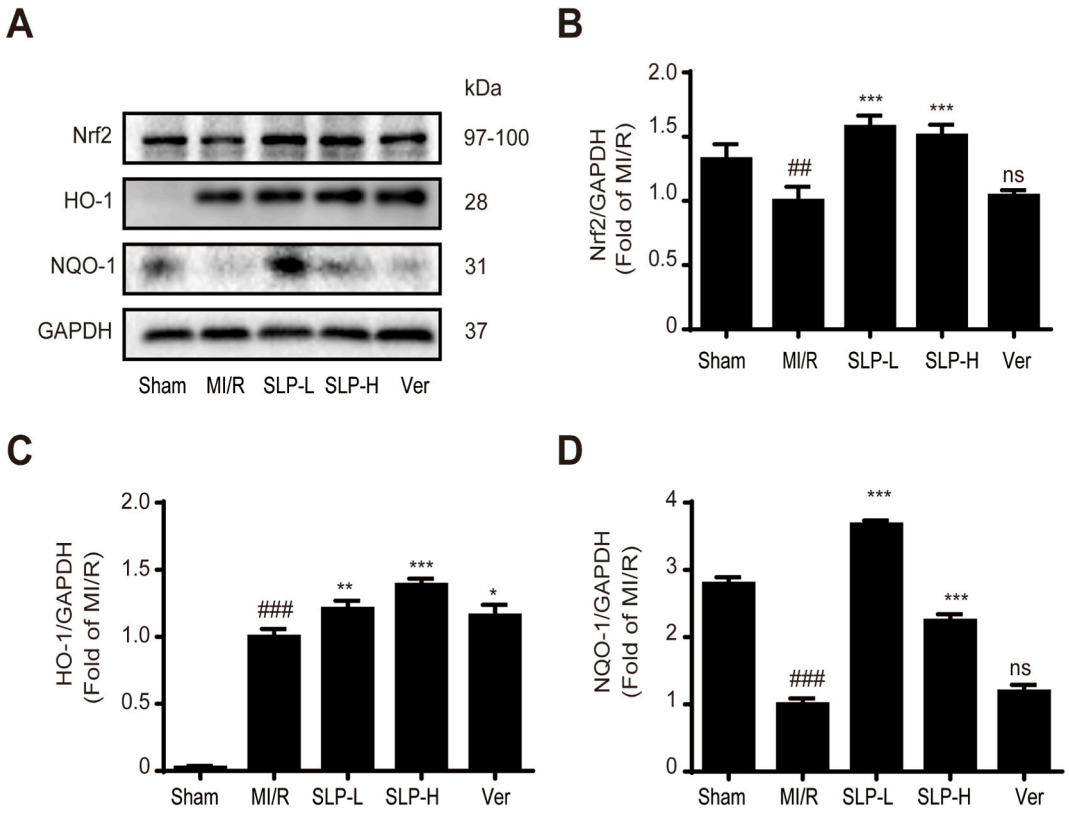

Fig. 8. SLP alleviated MI/R injury-induced oxidative stress by activating the Nrf2/HO-1 signaling pathway. After ischemia for 30 min and reperfusion induction for 2 h, the rat hearts were harvested and cryopreserved at −80 °C. To determine the related antioxidative proteins, the tissues were homogenized and the supernatant was collected. (A) The protein expression of Nrf2, HO-1, and NQO-1 was determined using western blotting. (B–D) Statistical analysis of the protein expression of Nrf2, HO-1, and NQO-1. n = 5, $^{\#\#}p < 0.01$, $^{\#\#\#}p < 0.001$, vs. the sham group. $^{ns}p > 0.05$, $^{*}p < 0.05$, $^{**}p < 0.01$, $^{***}p < 0.001$, vs. MI/R group.

and oxidative stress by activating Nrf2/HO-1 and inhibiting RIP1/RIP3/MLKL signaling pathways. In the *in vivo* experiment, SLP ameliorated MI/R injury by diminishing oxidative stress and necroptosis. These potential mechanisms of SLP indicated that oxidative stress and necroptosis may become a new focus of cardiovascular disease research and that SLP plays an important role in cardiovascular protection and has the potential to be developed as a new drug for the treatment of cardiovascular diseases.

Ethics statement

This study was reviewed and approved by the Ethics Committee on Laboratory Animal Management of Guangxi University of Chinese Medicine (approval number: DW20220526-115). The work has been carried out in accordance with either the U.K. Animals (Scientific Procedures) Act, 1986 and associated guidelines, the European Communities Council Directive 2010/63/EU or the National Institutes of Health – Office of Laboratory Animal Welfare policies and laws. All animal studies comply with the ARRIVE guidelines.

Consent for publication

We declare that the publisher has the authors' permission to publish the relevant contribution.

Data availability

All data generated or analyzed during this study are included in this published article.

CRediT authorship contribution statement

Kaili Sun: Investigation, Validation, Writing - original draft. **Renyikun Yuan:** Investigation, Resources, Visualization. **Jia He:** Investigation, Validation, Visualization. **Youqiong Zhuo:** Data curation, Visualization. **Ming Yang:** Methodology, Resources, Software. **Erwei Hao:** Resources, Software. **Xiaotao Hou:** Methodology, Resources. **Chun Yao:** Conceptualization, Supervision. **Shilin**

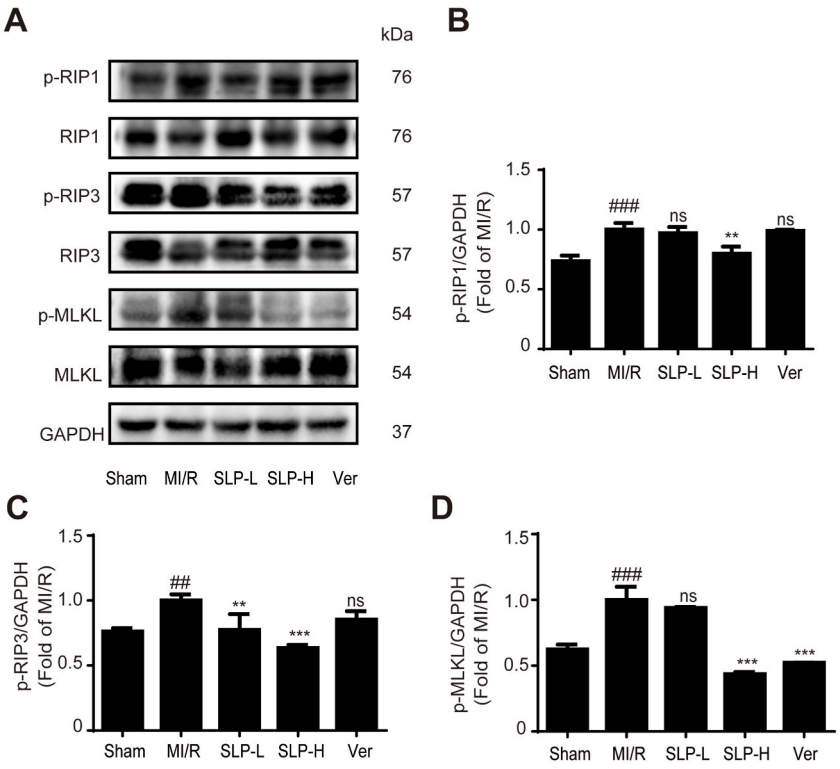

Fig. 9. SLP ameliorated MI/R injury-induced myocardial necroptosis by inhibiting the RIP1/RIP3/MLKL signaling pathway. After ischemia for 30 min and reperfusion induction for 2 h, the rat hearts were harvested and cryopreserved at −80 °C. To determine the related necroptosis proteins, the tissues were homogenized and the supernatant was collected. (A). The protein expressions of p-RIP1, RIP1, p-RIP3, RIP3, *p*-MLKL, and MLKL was measured using western blotting. (B–D) Statistical analysis of the protein expressions of p-RIP1, p-RIP3, and *p*-MLKL. n = 5, $^{\#\#}p < 0.01$, $^{\#\#\#}p < 0.001$, vs. the sham group. $^{ns}p > 0.05$, $^{*}p < 0.05$, $^{**}p < 0.01$, $^{***}p < 0.001$, vs. MI/R group.

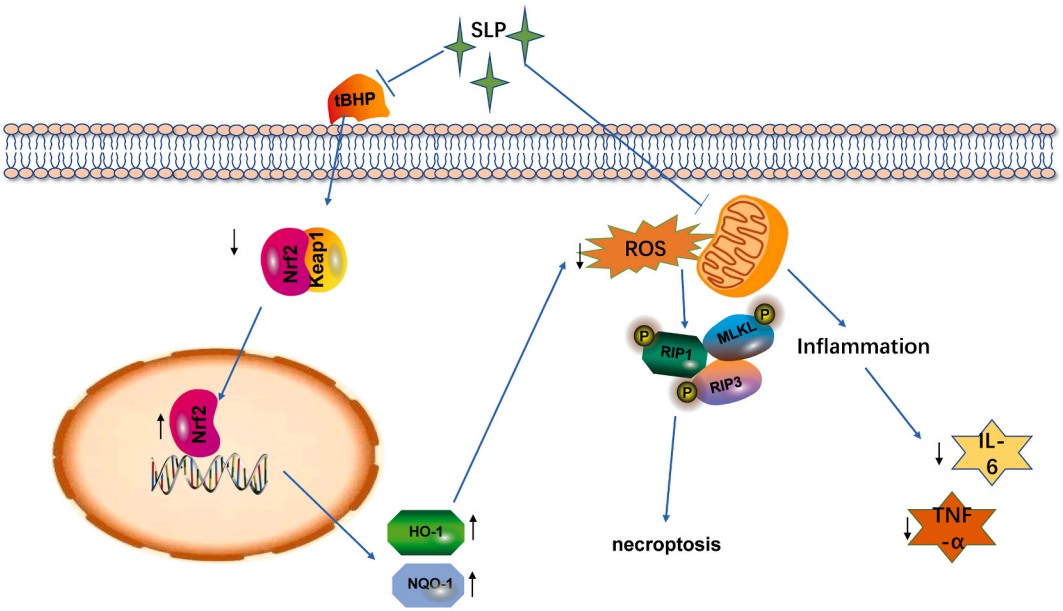

Fig. 10. Schematic diagram of the effects of SLP in cardiovascular protection. The mechanism of SLP in alleviating oxidative stress and necroptosis *in vitro* was through the Nrf2/HO-1 and RIP1/RIP3/MLKL signaling pathways.

Yang: Conceptualization, Supervision. **Hongwei Gao:** Conceptualization, Writing – review & editing.

Declaration of competing interest

The authors declare that they have no known competing financial interests or personal relationships that could have appeared to influence the work reported in this paper.

Acknowledgments

We appreciate the support from Qihuang High-level Talent Team Cultivation Project of Guangxi University of Chinese Medicine (2021002) and the National Natural Science Foundation of China (82060762).

References

[1] L.Y. Ma, W.W. Chen, R.L. Gao, et al., China cardiovascular diseases report 2018: an updated summary, J Geriatr Cardiol 1 (17) (2020) 1–8, https://doi.org/10.11909/j.issn.1671-5411.2020.01.001.
[2] Y. Gao, et al., Risk factors associated with recurrence within 90 days of ischemic stroke onset in Chinese medicine hospital: a national cross-sectional study in China, World J Tradit Chin Med 4 (6) (2020) 441–447, https://doi.org/10.4103/wjtcm.wjtcm_32_20.
[3] X. Zhang, H. Hu, J. Luo, et al., Ginsenoside Rb1 pretreatment attenuates myocardial ischemia by reducing calcium/calmodulin-dependent protein kinase II-medicated calcium release, World J Tradit Chin Med 3 (6) (2020) 284–294, https://doi.org/10.4103/wjtcm.wjtcm_24_20.
[4] X. Zhang, et al., A novel danshensu-tetramethylpyrazine conjugate DT-010 provides cardioprotection through the PGC-1α/Nrf2/HO-1 pathway, Biol. Pharm. Bull. 9 (40) (2017) 1490–1498, https://doi.org/10.1248/bpb.b17-00313.
[5] T. Hu, et al., Synergistic cardioprotective effects of Danshensu and hydroxysafflor yellow A against myocardial ischemia-reperfusion injury are mediated through the Akt/Nrf2/HO-1 pathway, Int. J. Mol. Med. 1 (38) (2016) 83–94, https://doi.org/10.3892/ijmm.2021.5045.
[6] C. Zhang, et al., Bisoprolol protects myocardium cells against ischemia/reperfusion injury by attenuating unfolded protein response in rats, Sci. Rep. 1 (7) (2017) 1–12, https://doi.org/10.1038/s41598-017-12366-8.
[7] J. Liu, H. Sui, J. Zhao, Y. Wang, Osmotin protects H9c2 cells from simulated ischemia-reperfusion injury through AdipoR1/PI3K/AKT signaling pathway, Front. Physiol. 8 (2017) 611, https://doi.org/10.3389/fphys.2017.00611.
[8] C. Sinning, D. Westermann, P. Clemmensen, Oxidative stress in ischemia and reperfusion: current concepts, novel ideas and future perspectives, Biomarkers Med. 11 (11) (2017) 11031–11040, https://doi.org/10.2217/bmm-2017-0110.
[9] S.H. Lim, J. Lee, Xyloglucan intake attenuates myocardial injury by inhibiting apoptosis and improving energy metabolism in a rat model of myocardial infarction, Nutr. Res. 45 (2017) 19–29, https://doi.org/10.1016/j.nutres.2017.07.003.
[10] S. Toldo, C. Marchetti, A.G. Mauro, et al., Inhibition of the NLRP3 inflammasome limits the inflammatory injury following myocardial ischemia–reperfusion in the mouse, Int. J. Cardiol. 209 (2016) 215–220, https://doi.org/10.1016/j.ijcard.2016.02.043.
[11] Y. Zhang, S.S. Su, S. Zhao, et al., RIP1 autophosphorylation is promoted by mitochondrial ROS and is essential for RIP3 recruitment into necrosome, Nat. Commun. 8 (2017), 14329, https://doi.org/10.1038/ncomms14329.
[12] S.-z. Wu, et al., Amifostine pretreatment attenuates myocardial ischemia/reperfusion injury by inhibiting apoptosis and oxidative stress, Oxid. Med. Cell. Longev. (2017), https://doi.org/10.1155/2017/4130824, 2017.
[13] Y.F. Liu, Y.Y. Chu, X.Z. Zhang, et al., TGFβ1 protects myocardium from apoptosis and oxidative damage after ischemia reperfusion, Eur. Rev. Med. Pharmacol. Sci. 7 (21) (2017) 1551–1558.
[14] R. Weinlich, A. Oberst, H.M. Beere, D.R. Green, Necroptosis in development, inflammation and disease, Nat. Rev. Mol. Cell Biol. 2 (18) (2017) 127–136, https://doi.org/10.1038/nrm.2016.149.
[15] W. Tonnus, et al., The pathological features of regulated necrosis, J. Pathol. 5 (247) (2019) 697–707, https://doi.org/10.1002/path.5248.
[16] H. Zhou, J. Ren, S. Toan, D. Mui, Role of mitochondrial quality surveillance in myocardial infarction: from bench to bedside, Ageing Res. Rev. 66 (2021), 101250, https://doi.org/10.1016/j.arr.2020.1012508.
[17] J.-M. Lv, M. Gouda, X.-Q. Ye, Z.-P. Shao, J.-C. Chen, Evaluation of proanthocyanidins from kiwi leaves (actinidia chinensis) against caco-2 cells oxidative stress through nrf2-ARE signaling pathway, Antioxidants 7 (11) (2022) 1367, https://doi.org/10.3390/antiox11071367.
[18] S. Fan, X. Liu, Y. Wang, et al., Thymus quinquecostatus Celak. ameliorates cerebral ischemia-reperfusion injury via dual antioxidant actions: activating Keap1/Nrf2/HO-1 signaling pathway and directly scavenging ROS, Phytomedicine 91 (2021), 153673, https://doi.org/10.1016/j.phymed.2021.153673.
[19] H.W. Li, T.J. Lan, C.X. Yun, et al., Mangiferin exerts neuroprotective activity against lead-induced toxicity and oxidative stress via Nrf2 pathway, Chin Herb Med 1 (12) (2019) 36–46, https://doi.org/10.1016/j.chmed.2019.12.002.
[20] Q. Su, L. Li, Y. Liu, Short-term effect of verapamil on coronary no-reflow associated with percutaneous coronary intervention in patients with acute coronary syndrome: a systematic review and meta-analysis of randomized controlled trials, Clin. Cardiol. 8 (36) (2013) E11–E16, https://doi.org/10.1002/clc.22143.
[21] M. Bao, W. Huang, Y. Zhao, et al., Verapamil alleviates myocardial ischemia/reperfusion injury by attenuating oxidative stress via activation of SIRT1, Front. Pharmacol. 13 (2022), 822640, https://doi.org/10.3389/fphar.2022.822640.
[22] Z. Huang, X. J, Model simulation of sugarcane yield in subtropical region of China, Chinese sugar 1 (2007) 5, https://doi.org/10.3969/j.issn.1007-2624.2007.01.003.
[23] M.J. Rao, M. Duan, J. Wang, et al., Transcriptomic and widely targeted metabolomic approach identified diverse group of bioactive compounds, antiradical activities, and their associated genes in six sugarcane varieties, Antioxidants 7 (11) (2022) 1319, https://doi.org/10.3390/antiox11071319.
[24] X.H. Liu, Extraction and content determination of polysaccharide in sugarcane leaves, Journal of Anhui Agricultural Sciences 34 (35) (2007) 10960, https://doi.org/10.1360/yc-007-0745, 10942.
[25] R. Colombo, F.M. Lanças, J.H. Yariwake, Determination of flavonoids in cultivated sugarcane leaves, bagasse, juice and in transgenic sugarcane by liquid chromatography-UV detection, J. Chromatogr. A 1 (1103) (2006) 118–124, https://doi.org/10.1016/j.chroma.2005.11.007.
[26] H. Trommer, R.H. Neubert, The examination of polysaccharides as potential antioxidative compounds for topical administration using a lipid model system, Int. J. Pharm. 1 (298) (2005) 153–163, https://doi.org/10.1016/j.ijpharm.2005.04.024.
[27] W.Y. Zhang Lijun Kx, Jincheng Li, Wenwei Lv, Therapeutic effect of sugarcane leaf polysaccharide on acute myocardial infarction model rats with blood stasis syndrome and its mechanism, Journal of Medicine of Yanbian University 3 (42) (2019) 4.
[28] T. Zavřel, P. Očenášová, M.A. Sinetova, J. Červený, Determination of storage (Starch/Glycogen) and total saccharides content in algae and cyanobacteria by a phenol-sulfuric acid method, Bio Protoc 15 (8) (2018), e2966, https://doi.org/10.21769/BioProtoc.2966.
[29] S.Y. Wan, J.G. Hu, Y. Zhang, et al., Recent advances of traditional Chinese medicine in the regulation of myocardial mitochondrial function, World J Tradit Chin Med 1 (2022) 8.
[30] S. Naaz, S. Mishra, P.K. Pal, A. Chattopadhyay, A.R. Das, D. Bandyopadhyay, Activation of SIRT1/PGC 1α/SIRT3 pathway by melatonin provides protection against mitochondrial dysfunction in isoproterenol induced myocardial injury, Heliyon 10 (6) (2020), e05159, https://doi.org/10.1016/j.heliyon.2020.e05159.
[31] E.A. Polyakova, E.N. Mikhaylov, M.M. Galagudza, E.V. Shlyakhto, Hyperleptinemia results in systemic inflammation and the exacerbation of ischemia-reperfusion myocardial injury, Heliyon 11 (7) (2021), e08491, https://doi.org/10.1016/j.heliyon.2021.e08491.

[32] F. Zeinali, A. Homaei, E. Kamrani, Identification and kinetic characterization of a novel superoxide dismutase from Avicennia marina: an antioxidant enzyme with unique features, J Biol Macromol 105 (2017) 1556–1562, https://doi.org/10.1016/j.ijbiomac.2017.07.054.
[33] F. Zeinali, A. Homaei, E. Kamrani, S. Patel, Use of Cu/Zn-superoxide dismutase tool for biomonitoring marine environment pollution in the Persian Gulf and the Gulf of Oman, Ecotoxicol. Environ. Saf. 151 (2018) 236–241, https://doi.org/10.1016/j.ecoenv.2018.01.029.
[34] R. Yuan, Y. Li, S. Han, et al., Fe-curcumin nanozyme-mediated reactive oxygen species scavenging and anti-inflammation for acute lung injury, ACS Cent. Sci. 8 (2022) 10–21, https://doi.org/10.1021/acscentsci.1c00866.
[35] Ma Ch, Chou Wc, Wu Ch, et al., Ginsenoside Rg3 attenuates TNF-α-induced damage in chondrocytes through regulating SIRT1-mediated anti-apoptotic and anti-inflammatory mechanisms, Antioxidants 12 (10) (2021) 1972, 10.3390/antiox1012197.
[36] W. Zhao, H. Feng, W. Sun, K. Liu, J.J. Lu, X. Chen, Tert-butyl hydroperoxide (t-BHP) induced apoptosis and necroptosis in endothelial cells: roles of NOX4 and mitochondrion, Redox Biol. 11 (2017) 524–534, https://doi.org/10.1016/j.redox.2016.12.036.
[37] S. Han, H. Gao, S. Chen, et al., Procyanidin A1 alleviates inflammatory response induced by LPS through NF-κB, MAPK, and Nrf2/HO-1 pathways in RAW264. 7 cells, Sci. Rep. 1 (9) (2019) 1–13, https://doi.org/10.1038/s41598-019-51614-x.
[38] T. Ali, T. Kim, S.U. Rehman, et al., Natural dietary supplementation of anthocyanins via PI3K/Akt/Nrf2/HO-1 pathways mitigate oxidative stress, neurodegeneration, and memory impairment in a mouse model of Alzheimer's disease, Mol. Neurobiol. 7 (55) (2018) 6076–6093, https://doi.org/10.1007/s12035-017-0798-6.
[39] S.T. Li, Q. Dai, S.X. Zhang, et al., Ulinastatin attenuates LPS-induced inflammation in mouse macrophage RAW264. 7 cells by inhibiting the JNK/NF-κB signaling pathway and activating the PI3K/Akt/Nrf2 pathway, Acta Pharmacol. Sin. 8 (39) (2018) 1294–1304, https://doi.org/10.1038/aps.2017.143.
[40] A. Loboda, M. Damulewicz, E. Pyza, A. Jozkowicz, J. Dulak, Role of Nrf2/HO-1 system in development, oxidative stress response and diseases: an evolutionarily conserved mechanism, Cell. Mol. Life Sci. 17 (73) (2016) 3221–3247, https://doi.org/10.1007/s00018-016-2223-0.
[41] X.S. Yang, T.L. Yi, S. Zhang, et al., Hypoxia-inducible factor-1 alpha is involved in RIP-induced necroptosis caused by in vitro and in vivo ischemic brain injury, Sci. Rep. 1 (7) (2017) 5818, https://doi.org/10.1038/s41598-017-06088-0.
[42] J. Chen, W.X. Fang, S.J. Li, et al., Protective effect of ginsenoside rd on lipopolysaccharide-induced acute lung injury through its anti-inflammatory and anti-oxidative activity, World Journal of Traditional Chinese Medicine 7 (2021) 383, https://doi.org/10.4103/wjtcm.wjtcm_12_21.
[43] C. Zhu, Z. Zuo, C. Xu, M. Ji, J. He, J. Li, Tumstatin (69-88) alleviates heart failure via attenuating oxidative stress in rats with myocardial infarction, Heliyon 9 (8) (2022), e10582, https://doi.org/10.1016/j.heliyon.2022.e10582.
[44] Y. Zhuo, R. Yuan, X. Chen, et al., Tanshinone I exerts cardiovascular protective effects in vivo and in vitro through inhibiting necroptosis via Akt/Nrf2 signaling pathway, Chin. Med. 1 (16) (2021) 1–15, https://doi.org/10.1186/s13020-021-00458-7.
[45] W. Zhou, J. Yuan, Necroptosis in health and diseases, Semin. Cell Dev. Biol. 35 (2014) 14–23, https://doi.org/10.1016/j.semcdb.2014.07.013.
[46] E.J. Lesnefsky, Q. Chen, B. Tandler, C.L. Hoppel, Mitochondrial dysfunction and myocardial ischemia-reperfusion: implications for novel therapies, Annu. Rev. Pharmacol. Toxicol. 57 (2017) 535–565, https://doi.org/10.1146/annurev-pharmtox-010715-103335.
[47] F. He, J. Li, Z. Liu, C.C. Chuang, W. Yang, L. Zuo, Redox mechanism of reactive oxygen species in exercise, Front. Physiol. 7 (2016) 486, https://doi.org/10.3389/fphys.2016.00486.
[48] M.R. Terluk, M.C. Ebeling, C.R. Fisher, et al., N-Acetyl-L-cysteine protects human retinal pigment epithelial cells from oxidative damage: implications for age-related macular degeneration, Oxid. Med. Cell. Longev. 2019 (2019), 5174957, https://doi.org/10.1155/2019/5174957.
[49] J. Zhao, S. Jitkaew, Z. Cai, et al., Mixed lineage kinase domain-like is a key receptor interacting protein 3 downstream component of TNF-induced necrosis, Proc. Natl. Acad. Sci. U.S.A. 14 (109) (2012) 5322–5327, https://doi.org/10.1073/pnas.1200012109.
[50] X. Gao, H. Zhang, W. Zhuang, et al., PEDF and PEDF-derived peptide 44mer protect cardiomyocytes against hypoxia-induced apoptosis and necroptosis via anti-oxidative effect, Sci. Rep. 4 (2014) 5637, https://doi.org/10.1038/srep05637.
[51] J.Y. Jia, E.H. Zang, L.J. Lv, et al., Flavonoids in myocardial ischemia-reperfusion injury: therapeutic effects and mechanisms, Chin Herb Med 1 (13) (2021) 49–63, https://doi.org/10.1016/j.chmed.2020.09.002.
[52] Y. Zhou, J. Zhang, B. Lei, et al., DADLE improves hepatic ischemia/reperfusion injury in mice via activation of the Nrf2/HO-1 pathway, Mol. Med. Rep. 5 (16) (2017) 6214–6221, https://doi.org/10.3892/mmr.2017.7393.
[53] Y. Ding, M. Chen, M. Wang, et al., Neuroprotection by acetyl-11-keto-β-boswellic acid, in ischemic brain injury involves the Nrf2/HO-1 defense pathway, Sci. Rep. 4 (2014) 7002, https://doi.org/10.1038/srep07002.
[54] Y. Jin, Z.L. Huang, L. Li, et al., Quercetin attenuates toosendanin-induced hepatotoxicity through inducing the Nrf2/GCL/GSH antioxidant signaling pathway, Acta Pharmacol. Sin. 1 (40) (2019) 75–85, https://doi.org/10.1038/s41401-018-0024-8.
[55] A. Koskela, F. Manai, F. Basagni, et al., Nature-inspired hybrids (NIH) improve proteostasis by activating nrf2-mediated protective pathways in retinal pigment epithelial cells, Antioxidants 7 (11) (2022) 1385, https://doi.org/10.3390/antiox11071385.